Sphingosine-1-phosphate receptor 2 is critical for follicular helper T cell retention in germinal centers

Saya Moriyama,[1,2,5] Noriko Takahashi,[1] Jesse A. Green,[6] Shohei Hori,[3] Masato Kubo,[4,8] Jason G. Cyster,[6,7] and Takaharu Okada[1,9,10]

[1]Laboratory for Tissue Dynamics, [2]Laboratory for Lymphocyte Differentiation, [3]Laboratory for Immune Homeostasis, and [4]Laboratory for Cytokine Regulation, RCAI, RIKEN Center for Integrative Medical Sciences (IMS-RCAI), Yokohama, Kanagawa 230-0045, Japan
[5]Graduate School of Frontier Biosciences, Osaka University, Suita, Osaka 565-0871, Japan
[6]Department of Microbiology and Immunology and [7]Howard Hughes Medical Institute, University of California, San Francisco, San Francisco, CA 94143
[8]Division of Molecular Pathology, Research Institute for Biomedical Science, Tokyo University of Science, Noda, Chiba 278-0022, Japan
[9]PRESTO, Japan Science and Technology Agency, Saitama, Saitama 332-0012, Japan
[10]Graduate School of Medical Life Science, Yokohama City University, Yokohama 230-0045, Japan

Follicular helper T (Tfh) cells access the B cell follicle to promote antibody responses and are particularly important for germinal center (GC) reactions. However, the molecular mechanisms of how Tfh cells are physically associated with GCs are incompletely understood. We report that the sphingosine-1-phosphate receptor 2 (S1PR2) gene is highly expressed in a subpopulation of Tfh cells that localizes in GCs. S1PR2-deficient Tfh cells exhibited reduced accumulation in GCs due to their impaired retention. T cells deficient in both S1PR2 and CXCR5 were ineffective in supporting GC responses compared with T cells deficient only in CXCR5. These results suggest that S1PR2 and CXCR5 cooperatively regulate localization of Tfh cells in GCs to support GC responses.

CORRESPONDENCE
Takaharu Okada:
tokada@rcai.riken.jp

Abbreviations used: CFP, cyan fluorescent protein; CGG, chicken gamma globulin; CMTMR,5-(and-6)-(((4-chloromethyl)benzoyl)amino)tetramethylrhodamine; FM, follicular mantle; GC, germinal center; HEL, hen egg lysozyme; NP, (4-hydroxy-3-nitrophenyl)acetyl; PP, Peyer's patch; S1PR2, sphingosine-1-phosphate receptor 2.

Follicular helper T (Tfh) cells are the helper T (Th) cell subset specialized in providing help to cognate antigen-specific B cells in the secondary lymphoid organs. Tfh cells develop in a manner dependent on the transcription factor Bcl6, and they express important molecules for shaping B cell responses such as IL-4, IL-21, CD40L, and PD-1 (Good-Jacobson et al., 2010; Kitano et al., 2011). Tfh cells are particularly important for the germinal center (GC) reaction that is essential for high affinity antibody production (Vinuesa et al., 2010) and is also thought to be important for the generation of immunological memory (McHeyzer-Williams et al., 2012).

Tfh cells access the B cell follicle by up-regulating CXCR5 and by down-regulating CCR7 (Haynes et al., 2007). In GC-containing follicles, Tfh cells are found both in the GC and the follicular mantle (FM), the outer follicle region surrounding the GC. Although some Tfh cells migrate between the GC and FM and between neighboring GCs, Tfh cells with the highest expression of PD-1 and CXCR5 appear to be preferentially accumulated in GCs (Linterman et al., 2012; Shulman et al., 2013). However, the mechanism of GC Tfh cell localization is incompletely understood. Because CXCR5 deficiency in T cells only mildly reduces the number of Th cells in the GC (Junt et al., 2005; Arnold et al., 2007; Haynes et al., 2007), other homing receptors are also likely to be involved in the GC Tfh cell localization.

Recently, it has been found that sphingosine-1-phosphate receptor 2 (S1PR2), a $G_{12/13}$-coupled receptor, is highly expressed in GC B cells and is involved in their clustering in the inner region of follicles (Green et al., 2011). Our previous microarray analysis showed that $CXCR5^{hi}PD\text{-}1^{hi}$ Tfh cells express modestly more *S1pr2* transcripts than $CXCR5^{lo}PD\text{-}1^{lo}$ Th cells (Kitano et al., 2011). In this study, using the *S1pr2*-reporter mice, we have demonstrated that *S1pr2* is expressed

The Rockefeller University Press $30.00
J. Exp. Med. 2014 Vol. 211 No. 7 1297-1305
www.jem.org/cgi/doi/10.1084/jem.20131666

The Journal of Experimental Medicine

at various levels in Tfh cells and that Tfh cells with high expression of *S1pr2* are retained in the GC in an S1PR2-dependent manner. Furthermore, we have shown that double deficiency of S1PR2 and CXCR5 in T cells severely impairs their localization to GCs and ability to support GC B cells, suggesting that S1PR2 plays a cooperative role with CXCR5 in Tfh cell biology.

RESULTS AND DISCUSSION

Regulatory effect of S1PR2 on Tfh cell migration in vitro

First, we tested for functional expression of S1PR2 in CXCR5^{hi}PD-1^{hi} Tfh cells by performing transwell migration analysis (Fig. 1 A). Migration of these cells toward CXCL13 and CXCL12 (Ansel et al., 1999) was suppressed by S1P. This suppression by S1P was reversed by treatment with the S1PR2 antagonist JTE-013, suggesting that the suppression was mediated by S1PR2. These results are consistent with the previously described function of S1PR2 that inhibits Rac-mediated chemotaxis by Rho activation (Skoura and Hla, 2009). In contrast, S1P rather induced migration of CXCR5^{-}CD4^{+} T cells, which was most likely mediated by G_i signaling-coupled S1P receptors, particularly S1PR1 (Matloubian et al., 2004). JTE-013 did not affect S1P- or CXCL12-induced migration of CXCR5^{-}CD4^{+} T cells, suggesting that S1PR2 expression is minimal in these cells.

Expression of *S1pr2* in Tfh cells

The modest *S1pr2* expression in Tfh cells, together with evidence that GC-associated Tfh cells differ phenotypically from non-GC–associated Tfh cells, led us to speculate that S1PR2 expression is enriched in a subfraction of CXCR5^{hi}PD-1^{hi} Tfh cells localized in GCs. To test this hypothesis, we generated a reporter mouse strain by gene targeting for detecting *S1pr2* expression in individual cells. A large portion of *S1pr2* gene protein coding region was replaced with the yellow fluorescent protein (*Venus*) gene (Fig. S1 A). Flow cytometry of Peyer's patch (PP) cells from *S1pr2*$^{Venus/+}$ (*S1pr2*$^{V/+}$) mice showed that GC B cells expressed uniformly high levels of Venus, and non-GC B cells were Venus negative (Fig. 1 B and Fig. S1 B). These observations are consistent with the previous reports (Cattoretti et al., 2009; Green et al., 2011). Within CD4^{+} T cell populations, the highest Venus signal was detected in Tfh cells, some of which expressed comparable levels of Venus as GC B cells. CXCR5^{int}PD-1^{int} Th cells expressed intermediate levels of Venus, and naive CD4^{+} T cells were Venus-negative (Fig. 1 B; and Fig. S1, B and C). Similar results were obtained for transferred *S1pr2*$^{V/+}$ OVA-specific TCR transgenic (OT-II) CD4^{+} T cells (unpublished data). Kinetics of Venus^{hi} OT-II Tfh cell development was slower than that of entire OT-II Tfh cell development, and was similar to that of GC B cell development (Fig. 1 C and Fig. S1 D). It has been recently found that FoxP3^{+} regulatory T cells also contain CXCR5^{hi}PD-1^{hi} cells, and these cells are called follicular regulatory T (Tfr) cells (Ramiscal and Vinuesa, 2013). Analysis of PP cells from *S1pr2*$^{V/+}$ mice that also carry the *Foxp3* reporter transgene (hCD2) showed that Tfr cells also expressed *S1pr2* (Fig. 1 D and Fig. S1 E). Tfr cells expressing *S1pr2* as highly as GC B cells were 22 ± 1.8% of Tfr cells, which was significantly lower than the percentage of *S1pr2*-high Tfh cells in Tfh cells (37 ± 2.1%, mean ± SEM, $n = 5$, $P = 0.0005$). These data suggest that Tfh cells and Tfr cells express various levels of S1PR2, and only subpopulations of these cells express S1PR2 as highly as GC B cells.

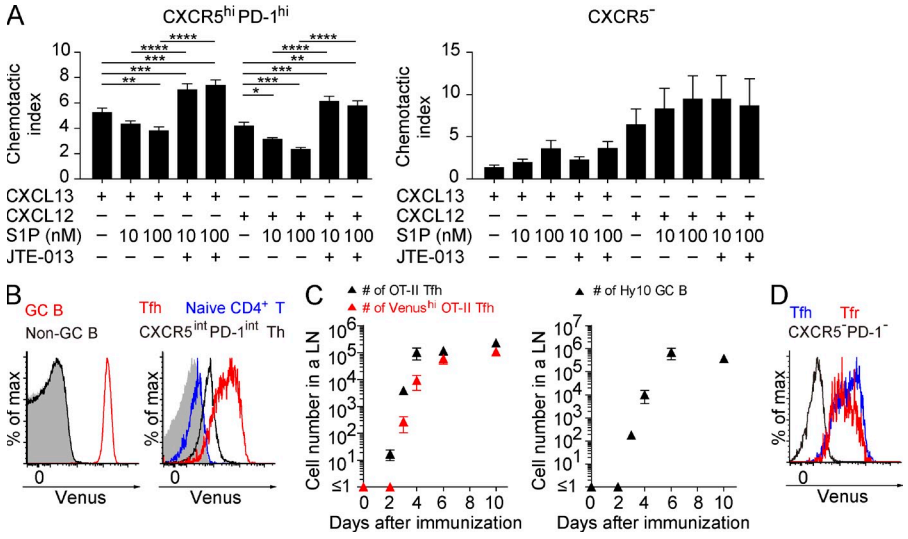

Figure 1. Functional expression of S1PR2 and magnitudes of *S1pr2* expression in CXCR5^{hi}PD-1^{hi} Tfh cells. (A) In vitro chemotaxis assay of CD4^{+} T cells. Splenocytes from mice 10–12 d after sheep red blood cell immunization were cultured in transwell plates and analyzed by flow cytometry. Chemotaxis of CXCR5^{hi}PD-1^{hi} and CXCR5^{-} CD4^{+} T cells was measured toward CXCL13 or CXCL12 with or without S1P and/or JTE-013. Data are pooled from three independent experiments and presented as mean ± SEM. $n = 8$–10. *, $P < 0.05$; **, $P < 0.01$; ***, $P < 0.001$; ****, $P < 0.0001$ (one-way ANOVA with Bonferroni's post-test). (B) Flow cytometric analysis of Venus expression on B cells (left) and CD4^{+} T cells (right) from PPs of *S1pr2*$^{V/+}$ mice. The gray filled histograms depict B cells or CD4^{+} T cells from *S1pr2*$^{+/+}$ mice. Data are representative of at least two independent experiments. (C) Developmental time course of Tfh cells and Venus^{hi} Tfh cells. *S1pr2*$^{V/+}$ OT-II T cells and Hy10 B cells (2×10^5 each per head) were cotransferred into recipient mice which were then immunized with HEL-OVA in CFA, and analyzed by flow cytometry on each time point. Total numbers of indicated donor cells in a draining LN are shown. Data are representative of two independent experiments, and presented as mean ± SEM. $n = 3$–7. (D) Flow cytometry data of PP CD4^{+} T cells from *Foxp3*^{hCD2} *S1pr2*$^{V/+}$ mice. Venus expression on indicated T cell subsets are shown. Data are representative of two independent experiments with five mice in total.

Tfh cells with high expression of *S1pr2* are localized in the GC in an S1PR2-dependent manner

To examine a role for S1PR2 in Tfh cell localization, histological analysis was performed. $S1pr2^{V/+}$ OT-II T cells were transferred to congenic recipient mice, and draining LNs were analyzed after immunization with (4-hydroxy-3-nitrophenyl)acetyl (NP) coupled to OVA (NP-OVA). 7 d after immunization, $S1pr2^{V/+}$ OT-II T cells expressing histologically detectable amounts of Venus were found mainly in the GC (Fig. 2 A). Venus expression levels in most of $S1pr2^{V/+}$ OT-II T cells in the FM and in the T cell zone were below the detection limit. In contrast, $S1pr2^{V/V}$ OT-II T cells expressing detectable amounts of Venus were not confined in the GC, and the majority of them were found in the FM but not in the T cell zone (Fig. 2 A). Interpretation of this observation requires caution because twice the number of the *Venus* transgenes can lead to an overestimation of the effect of S1PR2 deficiency. More importantly, however, the number of $S1pr2^{V/V}$ OT-II T cells in the GC was significantly reduced compared with $S1pr2^{+/+}$ OT-II T cells and $S1pr2^{V/+}$ OT-II T cells (Fig. 2, A and B) even though the formation of Tfh cells or expression of ICOS, Bcl6, and *Il21* was not significantly changed by S1PR2 deficiency (Fig. 2, C and D; and Fig. S2). Consistent with the previous report, S1PR2 deficiency augmented numbers of GC B cells in mucosal lymphoid organs, which contain chronic GCs (Green et al., 2011). However, Tfh cell numbers were not significantly changed by S1PR2 deficiency even in the mucosal lymphoid organs (unpublished data). These results strongly suggest that the S1PR2 expression does not affect the formation of Tfh cells but is important for their localization in the GC.

S1PR2 is important for retention of Tfh cells in the GC

To better understand the role for S1PR2 in Tfh cell dynamics in GC-containing follicles, we performed real-time two-photon microscopy. Avian-lysozyme–specific B cell receptor expressing Hy10 B cells harboring the cyan fluorescent protein (CFP) transgene and $S1pr2^{+/+}$ or $S1pr2^{V/V}$ OT-II T cells harboring the GFP transgene were transferred to recipient mice, and explanted LNs were observed 7 or 8 d after immunization with hen egg lysozyme (HEL) conjugated with OVA (HEL-OVA) in alum. GFP^+ OT-II T cells were visualized in follicles that contained GCs formed by CFP^+ Hy10 B cells (Fig. 3 A; and Videos 1 and 2). Centroids of OT-II T cells that came into the GC-FM interface zone were tracked to determine which side of the interface zone they migrated from and to (Video 3). A majority of $S1pr2^{+/+}$OT-II T cells that came from the GC to the interface zone were observed to

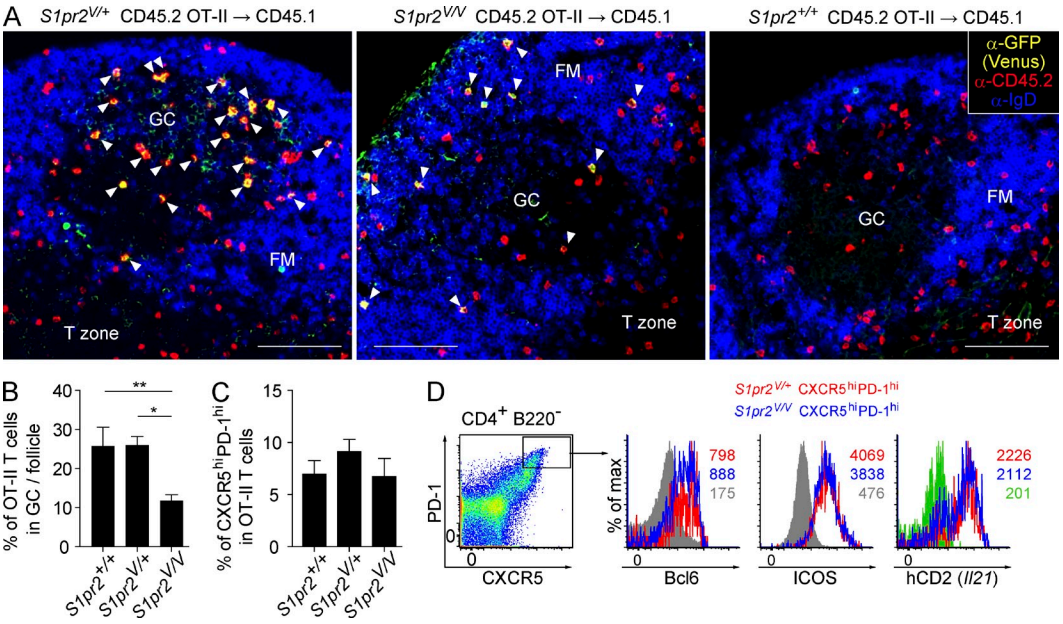

Figure 2. ***S1pr2*-high Tfh cells are localized in the GC in an S1PR2-dependent manner.** (A–C) OT-II T cells of the indicated genotypes were transferred to congenic recipient mice that were subsequently immunized with OVA in alum. Draining LNs were analyzed 7 d after immunization. Data are pooled from four (A and B) or three (C) independent experiments with 5–7 mice of each type in total. (A) Representative sections stained with anti-GFP antibody to detect Venus, for CD45.2 to identify OT-II T cells, and for IgD to demarcate GCs. OT-II T cells with clearly detectable levels of Venus expression are pointed with arrowheads. Bars, 100 µm. (B) Enumeration of the percentages of OT-II T cells in the GCs out of total OT-II T cells in the follicles. Data are normalized by the area of GCs and follicles, which was not significantly different between three groups, and presented as mean ± SEM of 9 ($S1pr2^{+/+}$), 7 ($S1pr2^{V/+}$), and 11 ($S1pr2^{V/V}$) different follicles. *, $P < 0.05$; **, $P < 0.01$ (one-way ANOVA with Bonferroni's post-test). (C) Flow cytometric enumeration of the percentages of Tfh cells in total OT-II T cell population. Data are presented as mean ± SEM. (D) Flow cytometry of Bcl6, ICOS, and *Il21* expression in Tfh cells of draining LN cells from mice of the indicated genotypes on 9 d after immunization. For *Il21* detection, mice were crossed with IL-21/hCD2 BAC transgenic mice. Gray- and green-filled histograms show the data of WT $CD44^{lo}$ $CD4^+$ T cells and WT Tfh cells, respectively. The left panel shows gating strategy for Tfh cells. Data are representative of two independent experiments with 3 (Bcl6 and ICOS) or 2 (*Il21*) mice of each genotype.

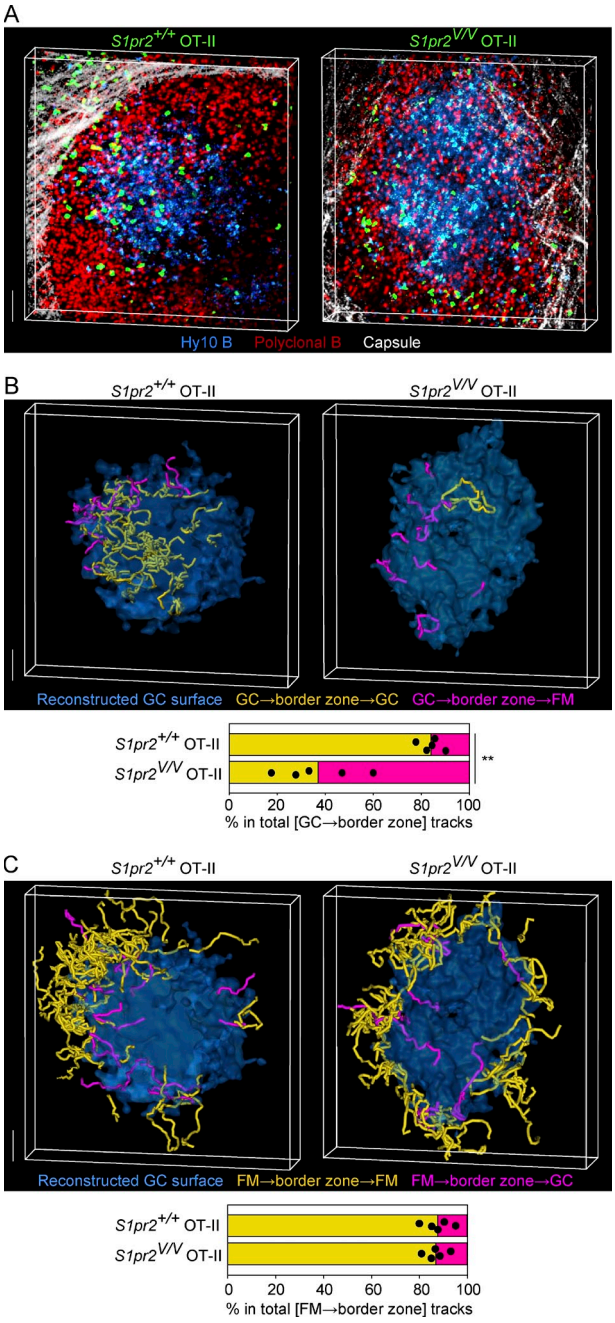

Figure 3. S1PR2 is important for Tfh cell retention in the GC. (A) Representative two-photon images of GCs. GFP$^+$ *S1pr2*$^{+/+}$ or GFP$^+$ *S1pr2*$^{V/V}$ OT-II T cells (2×10^4 cells per head), *S1pr2*$^{+/+}$ OT-II T cells (2×10^5 cells per head), and CFP$^+$ Hy10 B cells (2×10^5 cells per head) were transferred to recipient mice. Explanted LNs were observed 7 or 8 d after s.c. immunization with HEL-OVA in alum. 1–3 d before imaging, $1.4–3.0 \times 10^7$ rhodamine-labeled polyclonal B cells were transferred for demarcation of the follicular regions. See also Videos 1 and 2. The images are 84 µm (left) and 96 µm (right) z-projections. Data are representative of two independent experiments with 8 (*S1pr2*$^{+/+}$) and 5 (*S1pr2*$^{V/V}$) recipient mice in total. (B) Cell tracking analysis of OT-II T cells that access the interface zone from the GC. GC surfaces were reconstructed from the CFP images in A. The tracks show migration paths of OT-II T cells that entered the interface zone from the GC and then left the interface zone to the GC (yellow) or return to the GC, consistent with the previous report (Fig. 3 B; Qi et al., 2008). In contrast, *S1pr2*$^{V/V}$ OT-II T cells that came from the GC to the interface zone failed to show the preference for returning to the GC (Fig. 3 B). OT-II T cells that came from the FM to the interface zone showed a clear preference for returning to the FM, regardless of their genotype (Fig. 3 C). These results, together with the flow cytometry data (Fig. 1) and the histological data (Fig. 2), suggest that S1PR2 is important for retaining the S1PR2^{hi} subpopulation of Tfh cells in the GC.

Tfh cells with high expression of *S1pr2* most abundantly express the key genes for Tfh cell function

To further characterize the Tfh cell subpopulations expressing different levels of *S1pr2*, we sorted Venus^{hi} Tfh cells, Venus^{lo} Tfh cells, PD-1^{int} Th cells, PD-1^{lo} Th cells, and naive CD4$^+$ T cells (Fig. S3 A) and compared their mRNA expression profiles by microarray analysis (Fig. 4 A). Although Venus^{hi} Tfh cells and Venus^{lo} Tfh cells showed generally similar gene expression profiles, there were several notable differences. *Bcl6* expression was higher in Venus^{hi} Tfh cells than in Venus^{lo} Tfh cells and in PD-1^{int} Th cells. *Ccr7* expression was low but still detectable in Venus^{lo} Tfh cells, whereas it was virtually abrogated in Venus^{hi} Tfh cells. Expression of several other G_i–coupled receptor genes, *Ccr6*, *Gpr18*, *Gpr183*, and *S1pr1*, was lower in Venus^{hi} Tfh cells than in Venus^{lo} Tfh cells, which might redundantly contribute to the segregation of Venus^{hi} Tfh cells in the GC and Venus^{lo} Tfh cells in the FM. Microarray data showed that Venus^{hi} Tfh cells expressed slightly more transcripts of *Il4* (1.41-fold) and *Il21* (1.23-fold) than Venus^{lo} Tfh cells. To more clearly address these points, we crossed the *S1pr2*^{Venus} mice with two different reporter mouse strains to detect *Il4* or *Il21* expression. Consistent with the previous reports, expression of the *Il4* and *Il21* reporters (human CD2) was detected selectively in Tfh cells (Reinhardt et al., 2009; Harada et al., 2012; Lüthje et al., 2012; Fig. S3 B). Within Tfh cells, the percentage of cells expressing the *Il4* and *Il21* reporters was higher in the Venus^{hi} population (Fig. 4, B and C; Fig. S3 C). These results suggest that S1PR2^{hi} Tfh cells most abundantly express the important molecules for Tfh cell function.

FM (pink). The color brightness of the tracks is reduced on the parts submerged under the GC surfaces. The horizontal histogram shows the ratios of yellow tracks to pink tracks. Dots represent individual LNs used for the imaging analysis. 6–79 cells were tracked per LN. **, $P < 0.01$ (Student's *t* test). (C) Cell tracking analysis data of OT-II T cells that access the interface zone from the FM. The tracks show migration paths of OT-II T cells that entered the interface zone from the FM and then left the interface zone to the FM (yellow) or GC (pink). The graph shows the ratios of yellow tracks to pink tracks. 12–98 cells were tracked per LN. Bars, 50 µm. Data are pooled from two independent experiments with 8 (*S1pr2*$^{+/+}$) and 4 (*S1pr2*$^{V/V}$) mice in total (B and C).

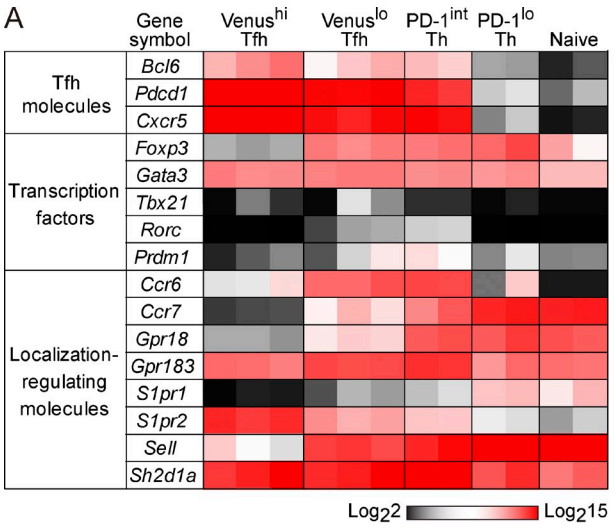

Figure 4. mRNA expression profiles of Tfh cells with different levels of *S1pr2* expression. (A) mRNA expression profiles of Venus^{hi} Tfh, Venus^{lo} Tfh, PD-1^{int} Th, PD-1^{lo} Th, and naive CD4$^+$ T cells are shown as heat map. See Fig. S3 A for the details of cell sorting. Each column represents a single experiment pooled from 3 to 8 (Venus^{hi} Tfh, Venus^{lo} Tfh, PD-1^{int} Th, PD-1^{lo} Th) or 1 to 2 (naive CD4$^+$ T) mice. (B and C) The cytokine reporter (hCD2)–expressing cell percentages in Venus^{lo} or Venus^{hi} Tfh cells of *S1pr2$^{V/+}$Il4*-reporter mice (B) and *S1pr2$^{V/+}$Il21*-reporter mice (C). Draining LN cells were analyzed 9 or 11 d after immunization with CGG in CFA s.c. Data are pooled from two independent experiments with 8 LNs from 2 mice (B) or 7 LNs from 2 mice (C). Horizontal bars represent mean values. ***, $P < 0.001$; ****, $P < 0.0001$ (Student's *t* test).

Requirements for S1PR2 and CXCR5 in Tfh cells to support GC responses

Because S1PR2 deficiency reduced the number of Tfh cells in GCs by half (Fig. 2 B), we sought to investigate its impact on GC responses. To eliminate the effects of S1PR2 deficiency in B cells (Green et al., 2011), *S1pr2$^{V/V}$* or control CD4$^+$ T cells were transferred to *Cd28$^{-/-}$* mice, which have a much reduced number of Tfh cells (Linterman et al., 2009), and analyzed after immunization. As shown in Fig. 5 A, *S1pr2$^{V/V}$* and control CD4$^+$ T cells could similarly support GC B cells. Histological analysis showed that the number of CD4$^+$ T cells in GCs was significantly reduced in *S1pr2$^{V/V}$*

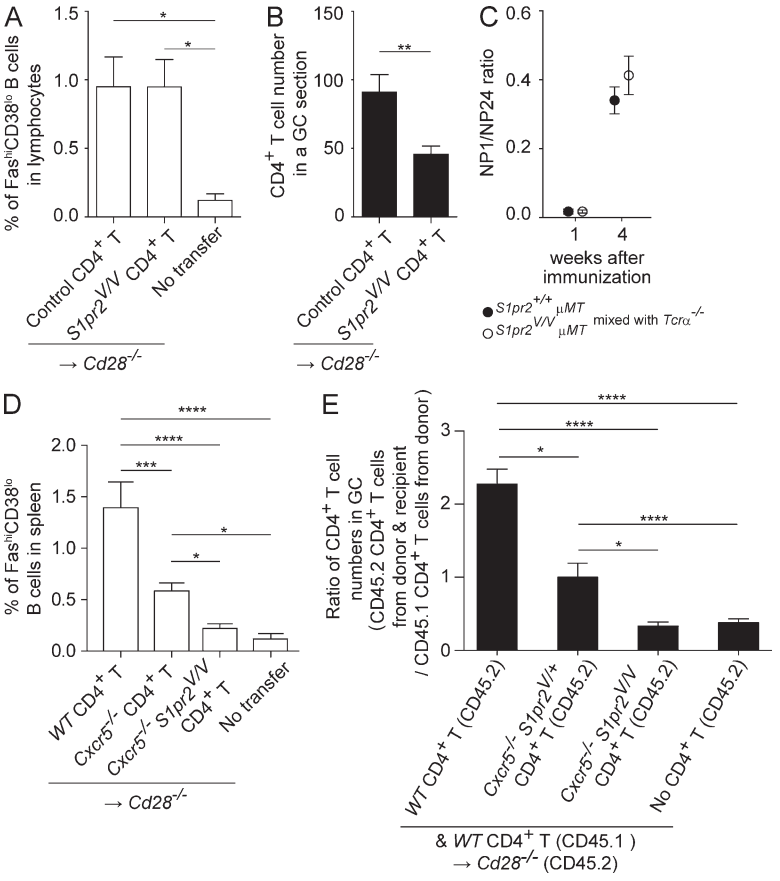

Figure 5. S1PR2 and CXCR5 expression in Tfh cells are required for supporting GC responses. (A and B) *S1pr2$^{+/+}$* or *S1pr2$^{V/+}$* (control), or *S1pr2$^{V/V}$* CD4$^+$ T cells were transferred to *CD28$^{-/-}$* mice, and mice were immunized with NP-CGG in alum or CFA and analyzed 2 wk after immunization. Data are pooled from three independent experiments. (A) Flow cytometric enumeration of the percentages of GC cells in lymphocytes. $n = 6$ (control), 6 (*S1pr2$^{V/V}$*), and 4 (no transfer control). Data are presented as mean ± SEM. (B) Enumeration of CD4$^+$ T cell number in GC sections. 22 GCs from 5 mice (control) and 24 GCs from 5 mice (*S1pr2$^{V/V}$*) were analyzed. Data are presented as mean ± SEM. (C) ELISA data of sera collected from mixed BM chimeras of indicated genotypes. Sublethally irradiated Rag1-deficient mice were reconstituted with *S1pr2$^{+/+}$* μMT BM cells or *S1pr2$^{V/V}$* μMT BM cells mixed with *Tcrα$^{-/-}$* BM cells, and immunized i.p. with NP-CGG in alum. Ratios of anti-NP1 IgG1 concentration to anti-NP24 IgG1 concentration are shown. Data are representative of three independent experiments, and are presented as mean ± SEM. $n = 4$ (*S1pr2$^{+/+}$* μMT) and 4 (*S1pr2$^{V/V}$* μMT). (D) CD4$^+$ T cells of the indicated genotypes were transferred to *Cd28$^{-/-}$* mice. On the next day, the mice were immunized i.p. with NP-OVA in alum, and GC B cell frequencies were analyzed 3 wk after immunization by flow cytometry. Data are pooled from three independent experiments, and are presented as mean ± SEM. $n = 6$ (*Cxcr5$^{-/-}$*), 7 (*Cxcr5$^{-/-}$ S1pr2$^{V/V}$*), 5 (WT), and 3 (no transfer control). (E) CD4$^+$ T cells were mixed in 1: 1 ratio, and transferred to *Cd28$^{-/-}$* mice. On the next day, the mice were immunized i.p. with NP-OVA in alum, and analyzed 3 wk after immunization. Data are representative of two experiments, and are presented as mean ± SEM. Shown is the number of CD45.2 CD4$^+$ T cells in GC sections normalized by the number of CD45.1 CD4$^+$ T cells in GC sections. 9 different GCs from 2 mice were analyzed for each donor type. *, $P < 0.05$; **, $P < 0.01$; ***, $P < 0.001$; ****, $P < 0.0001$ (A, B, D, and E). One-way ANOVA with Bonferroni's post-test (A, D, and E) and Student's *t* test (B) were used for statistical analysis.

$CD4^+$ T cell–transferred mice compared with control $CD4^+$ T cell–transferred mice, consistent with the data shown in Fig. 2 B (Fig. 5 B and Fig. S4 A). The area of a GC section was not significantly different between two groups (Fig. S4 B). The ratio of $CXCR5^{hi}$ Tfh/GC B cell numbers was not affected by S1PR2 deficiency in T cells, indicating that total Tfh cell formation was unaffected (Fig. S4 C). We also observed similar GC formation between two groups of sublethally irradiated Rag1-deficient mice, one group reconstituted with $S1pr2^{+/+}$ μMT BM cells mixed with $Tcr\alpha^{-/-}$ BM cells and the other reconstituted with $S1pr2^{V/V}$ μMT BM cells mixed with $Tcr\alpha^{-/-}$ BM cells, after immunization with NP–chicken gamma globulin (CGG) in alum i.p. (unpublished data). In addition, both chimera types produced similar amounts of anti-NP1 and NP24 IgG1, and the ratio of NP1/NP24 was comparable (Fig. 5 C and Fig. S4 D). These results suggest that, contrary to our expectations, the partial decrease of GC Tfh cells caused by S1PR2 deficiency alone may not significantly affect GC B cell maintenance at least in these experimental settings. Because previous studies showed that T cell–specific CXCR5 deficiency only mildly reduced GC responses (Junt et al., 2005; Arnold et al., 2007; Haynes et al., 2007), we next examined if deficiency of both CXCR5 and S1PR2 in Th cells would further suppress GC responses. WT, $Cxcr5^{-/-}$, or $Cxcr5^{-/-}$ $S1pr2^{V/V}$ $CD4^+$ T cells were transferred to $Cd28^{-/-}$ mice, and the percentage of GC B cells was examined after immunization. In agreement with the previous studies, GC B cell formation supported by $Cxcr5^{-/-}$ $CD4^+$ T cells was partially impaired compared with that supported by WT $CD4^+$ T cells (Arnold et al., 2007; Haynes et al., 2007). Strikingly, GC responses were further reduced when the transferred $CD4^+$ T cells lacked both CXCR5 and S1PR2 (Fig. 5 D). Percentages of activated cells in transferred $CD4^+$ T cells of the individual genotypes were not significantly different, suggesting that priming of S1PR2 and CXCR5 double-deficient $CD4^+$ T cells occurred normally (Fig. S4 E). Histological analysis confirmed that GCs supported by CXCR5 and S1PR2 double-deficient T cells were hypoplastic and scarcely even contained T cells compared with GCs supported by CXCR5 single-deficient T cells (unpublished data). These results strongly suggest that S1PR2 in Tfh cells has a cooperative role with CXCR5 in supporting GC responses.

S1PR2 and CXCR5 play cooperative roles for GC Tfh cell localization

To quantitatively determine the effect of S1PR2 and CXCR5 double deficiency on T cell localization in well-formed GCs, we cotransferred CD45.1 WT $CD4^+$ T cells with CD45.2 WT, $Cxcr5^{-/-}$ $S1pr2^{V/+}$, or $Cxcr5^{-/-}$ $S1pr2^{V/V}$ $CD4^+$ T cells to $Cd28^{-/-}$ mice, and immunized the mice. Histological analysis revealed that the number of CD45.2 $CD4^+$ T cells in GCs relative to the number of CD45.1 $CD4^+$ T cells in GCs was decreased when transferred CD45.2 $CD4^+$ T cells were CXCR5-deficient, and was even further reduced when transferred CD45.2 $CD4^+$ T cells were S1PR2 and CXCR5 double-deficient (Fig. 5 E, and Fig. S4 F). These results, together with the results shown in Figs. 2 and 3, strongly suggest that S1PR2 and CXCR5 in Tfh cells act additively and are required for their localization in GCs.

In essence, our data indicate that GC Tfh cells are retained within GCs by means of their S1PR2 expression. S1PR2 has been previously shown to contribute to accumulation of GC B cells in the central region of the follicle (Green et al., 2011; Wang et al., 2011). This is most likely mediated by negative concentration gradients of S1P from the perimeter to the center of the follicle, established through the actions of S1P degrading enzymes (Green and Cyster, 2012). In addition to retention in GCs, it is possible that S1PR2 may promote Tfh cell recruitment to GCs if they start to express S1PR2 while they are outside of GCs. Our analysis also shows that S1PR2 mediates CXCR5-independent GC association of T cells. We speculate that S1P concentration may be lower in the GC than in the T cell zone, and that CXCR5-deficient Th cells that have down-regulated CCR7 enter follicles at a relatively low frequency, after which some of them may be retained in GCs due to the S1PR2-mediated inhibition of migration back to the T cell zone.

A very recent study using the in vivo photoconversion technique has shown that although Tfh cells become concentrated in GCs over time, they can exchange between GCs within a responding LN (Shulman et al., 2013). After 20 h, about one third of photoconverted Tfh cells from a single GC were found in neighboring follicles and other GCs. This indicates a residence half-time in a given GC exceeding 1 d, considerably longer than the residence half-time of naive T cells in an entire LN (Lo et al., 2005). Given the small size of the GC structure, these data are consistent with strong confinement of most GC Tfh cells to the GC. It will be important in future work to assess if GC Tfh cells down-modulate S1PR2 expression over the course of immune response or in response to antigen boost to increase the extent of exchange between GCs.

Our data have demonstrated that GC formation is severely impaired when T cells lack not only CXCR5 but also S1PR2, suggesting that S1PR2-mediated Tfh cell retention in GCs contributes to the maintenance of GC responses. At this point, however, it is not excluded that possible additional roles of S1PR2 signaling in Tfh cells may also contribute to GC responses, as S1PR2 signaling in GC B cells regulates not only their localization but also their survival.

The present study demonstrates the cooperative interplay between CXCR5 and S1PR2 for Tfh cells to promote GC responses, which exemplifies that a G_i-coupled receptor and a $G_{12/13}$-coupled receptor can work redundantly for cells to exert their function in vivo. Nonetheless, it is still possible that S1PR2 in Tfh cells has nonredundant roles for GC responses. As S1PR2 deficiency in T cells is likely to reduce the number of GC Tfr cells, which may counteract the effect of the partial reduction of GC Tfh cells (Ramiscal and Vinuesa, 2013), it will be important to test the outcome of Tfh cell–specific S1PR2 deficiency. Future studies will also need to test the

impact of S1PR2 deficiency in T cells on long-term antibody responses against viruses and on antibody diversification to maintain balanced microbiota in the gut.

MATERIALS AND METHODS

Mice. To generate the *S1pr2*^{Venus} mice, the first 498 bp of the *S1pr2* protein coding region was replaced with the *Venus* gene. A loxP-flanked PGK-Neo cassette was inserted before exon 2, a 7.1-kb fragment was used as the 5′ homology region, and a 2-kb fragment was used as the 3′ homology region. C57BL/6J × C57BL/6N hybrid ES cells were transfected, cultured, and selected. Then, correctly targeted clones were aggregated with BALB/c morulas. Chimeric male offspring were mated with C57BL/6J female mice, and their offspring were mated with CAG-Cre transgenic mice to excise the PGK-Neo cassette. Approximately 40% of *S1pr2*$^{V/V}$ mice at the age of 3–5 wk were found dead, often in seizure-like postures as previously described for the other S1PR2-deficient mouse lines (MacLennan et al., 2001; Du et al., 2010). C57BL/6J mice were purchased from CLEA Japan. Rag1-deficient mice were bred and maintained in CLEA Japan. β-actin–CFP (The Jackson Laboratory), CD28-deficient (The Jackson Laboratory), CD45.1 congenic (The Jackson Laboratory), CXCR5-deficient (The Jackson Laboratory), *Foxp3*^{hCD2} (Miyao et al., 2012), HEL-specific Ig–knock-in Hy10 (previously named VDJ9/κ5; Allen et al., 2007), IL-4/hCD2 transgenic, IL-21/hCD2 transgenic (Harada et al., 2012), μMT (The Jackson Laboratory), OT-II (The Jackson Laboratory), TCR-α–deficient (The Jackson Laboratory; Mombaerts et al., 1992), and UBC-GFP (The Jackson Laboratory) mice were bred and maintained in specific pathogen-free conditions at the animal facility of RIKEN Center of Integrative Medical Sciences. For BM reconstitution, BM cells were injected i.v. to 6 Gray-irradiated Rag1-deficient mice, and the mice were immunized 3 mo after reconstitution. All animal studies were performed in accordance with the guidelines of the RIKEN Animal Research Committee and were conducted under protocols approved by the Animal Experiments Committee of RIKEN Yokohama Institute.

Cell isolation, adoptive transfer, and immunization. Splenocytes, LN cells, and PP cells were harvested by mechanical disruption with slides (Matsunami Glass) or on 40-μm nylon cell strainers (BD) in DMEM containing 2% FBS. BM cells were flushed from femurs and tibiae in DMEM containing 2% FBS. After removal of red blood cells if necessary, non-CD4$^+$ cells were labeled with biotinylated anti-B220 (RA3-6B2), anti-CD8a (53–6.7), anti-CD11b (M1/70.15), anti-CD11c (HL3), anti–Gr-1 (RB6-8C5), and anti-NK1.1 (PK136), followed by Streptavidin MicroBeads (Miltenyi Biotec). Non–B cells were directly labeled with CD43 MicroBeads (Miltenyi Biotec). Samples were magnetically depleted of labeled cells with the autoMACS cell separator (Miltenyi Biotec) or using CS columns (Miltenyi Biotec), and the purity of CD4$^+$ T cells and B220$^+$ B cells was typically >80% and >95%, respectively. For two-photon imaging, purified B cells were labeled with 20 μM 5-(and-6)-(((4-chloromethyl)benzoyl)amino)tetramethylrhodamine (CMTMR; Invitrogen) in DMEM containing 2% FBS for 20 min at 37°C. 1–3 d before imaging, 1.4–3.0 × 10^7 CMTMR-labeled polyclonal B cells were transferred i.v. In most experiments, 1–5 × 10^5 Ag-specific T cells and B cells were transferred. The next day, the mice were immunized s.c. in the footpad, base of the tail, flank, and scruff with 10–15 μg NP(16)-OVA (Bioresearch Technologies), HEL-OVA, CGG (EMD Millipore), or NP-CGG mixed in alum (Imject alum; Thermo Fisher Scientific) or CFA (Sigma-Aldrich) per site. For the time course experiment, *S1pr2*$^{V/+}$ OT-II T cells and Hy10 B cells (2 × 10^5 each per head) were cotransferred into recipient mice which were then s.c. immunized with HEL-OVA in CFA 1 d after cell transfer. The results about flow cytometry patterns of *S1pr2*-Venus versus CXCR5/PD-1 are very similar between CFA immunization and alum immunization.

Two-photon microscopy and image analysis. Explanted LNs were imaged as previously described (Kitano et al., 2011). Multiphoton excitation was provided by a Mai Tai HP Ti:Sapphire laser (Spectra Physics) tuned to 900 nm, and images were acquired with a 20×/1.00 NA water immersion objective (Leica). Clusters of CFP$^+$ Hy10 B cells in which transferred CMTMR-labeled polyclonal B cells were apparently sparse compared with the region outside the clusters were used as the GC region for subsequent analysis. Areas within 10 μm of the GC surface reconstructed from CFP$^+$ B cell clusters were defined as the GC-FM interface zone. T cell tracking and the creation of GC surface were performed using Imaris 64× 7.2.3 (Bitplane) tracking and surface command. Tracks (>8 min) of T cells that moved into and then left the GC-FM interface zone were used for quantitative analysis.

Flow cytometry. The cells were stained anti-B220 (RA3-6B2, APC/Cy7), anti-Bcl6 (K112-91, PE), anti-CD4 (RM4-5, PE/Cy7 and PerCP-Cy5.5), anti-CD38 (90, APC), anti-CD44 (IM7, APC/Cy7 and PE/Cy7), anti-CD45.1 (A20; PerCP-Cy5.5, Pacific blue and APC/Cy7), anti-CD45.2 (104, Pacific blue and PE), anti-CD62L (MEL-14, APC and PerCP-Cy5.5), anti-CD95 (Jo2, PE/Cy7), anti–human CD2 (RPA-2.10, PE), anti-CXCR5 (2G8, APC), anti-IgD (11-26c, eFluor450), anti-ICOS (15F9, PE), anti–Ly-77 (GL7, biotin), anti–PD-1 (J43, PE), and streptavidin reagents (Pacific blue, APC, PE and PerCP-Cy5.5) and analyzed on a FACSCanto II (BD). Bcl6 staining was performed as previously described (Kitano et al., 2011). Antibodies were purchased from BD, BioLegend, or eBioscience. The data were analyzed with FlowJo software (Tree Star).

Immunofluorescence microscopy. Draining LNs and spleens were fixed with 4% paraformaldehyde, washed with PBS, and then placed in Tissue-Tek OCT compound (Sakura) and snap-frozen in dry ice and ethanol. Cryosections 8 μm in thickness were affixed to MAS-GP–coated slides (Matsunami Glass) and stained at room temperature for 2 h or at 4°C for overnight with anti-IgD (11-26c.2a, FITC and PE), anti-CD4 (RM4-5, PE), anti-CD45.1 (A20, APC), anti-CD45.2 (104, APC), and rabbit anti–Bcl-6 (N-3; Santa Cruz Biotechnology, Inc.), which was detected by FITC-conjugated goat anti–rabbit IgG (SouthernBiotech) or by Alexa Fluor 488–conjugated goat anti–rabbit IgG (Invitrogen). Some samples were dehydrated with ethanol after sectioning instead of 4% paraformaldehyde fixation. Venus expression was detected by goat anti-GFP antibody (Rockland), biotinylated donkey anti–goat IgG antibody (Jackson ImmunoResearch Laboratories, Inc.), and TSA kit with HRP-streptavidin and Alexa Fluor 488 or Alexa Fluor 546 tyramide (Invitrogen). Images were acquired on BZ-9000 (Keyence), and processed with Photoshop (CS5.1; Adobe). ImageJ (National Institutes of Health) was used for the measurement of follicle and GC area for normalization of Tfh cell counts.

Microarray. Total RNA was isolated from FACSAria II (BD)–sorted T cells using TRIzol reagent (Invitrogen). Biotinylated cDNA was synthesized using the Ovation RNA Amplification System V2 (Nugen) and FL-Ovation cDNA Biotin Module V2 (Nugen), and then hybridized with Mouse Genome 430 2.0 Arrays (Affymetrix). Expression values for each probe set were calculated with the GC-RMA method in the GeneSpring GX 7.3 software package (Agilent Technologies).

Cell migration assay. Splenic CD4$^+$ T cells were prepared from C57BL/6 mice 10–12 d after sheep red blood cell immunization, and resensitized for 40 min at 37°C before adding to 5 μm transwells. 1 μg/ml CXCL13 (R&D Systems), 250 ng/ml CXCL12 (PeproTech), 10 μM JTE-013 (Tocris Bioscience), and S1P (Sigma-Aldrich) was added to the lower chamber as indicated in the figure, and analyzed as previously described (Green et al., 2011). In our experiments, 20–35% of input CXCR5^{hi} T cells migrated in response to CXCL13, and 4–6% of input CXCR5^{hi} T cells migrated without chemokines. To calculate the chemotactic index, the number of cells that migrated in response to chemokines and S1P was divided by the number of cells that migrated without chemokines or S1P.

ELISA. 96-well plates (Thermo Fisher Scientific) were coated overnight at 4°C with 2 μg/ml NP1-BSA or NP24-BSA diluted with borate-buffered saline. After washing, PBS containing 0.5% BSA and 0.05% Tween-20 was added to the plates to prevent nonspecific binding. Then, serial dilutions of

sera and anti-NP monoclonal antibody standard (C6) were applied to the plates for 2 h at room temperature. After washing, HRP-conjugated goat anti–mouse IgG1 antibody (Southern Biotech) was applied to the plates for 2 h at room temperature. Bound secondary antibodies were detected by incubation with SureBlue TMB 1–Component Microwell Peroxidase Substrate (KPL). The concentration of anti-NP antibodies was calculated by standard curve.

Statistical analysis. Means of two groups were compared with nonpaired two-tailed Student's *t* test, and means between three or more groups were compared with one-way ANOVA with Bonferroni's post-test using Prism software (GraphPad Software).

Accession number. All microarray data are available in the Gene Expression Omnibus (GEO) database under accession no. GSE56883.

Online supplemental material. Fig. S1 shows generation of the *S1pr2*^{Venus} mice, and representative flow cytometry plots and gating strategy for the data shown in Fig. 1 (B–D). Fig. S2 shows representative flow cytometry plots and gating strategy for the data shown in Fig. 2 C. Fig. S3 shows gating strategy and representative flow cytometry plots for the data shown in Fig. 4. Fig. S4 shows representative histological images and supporting data for Fig. 5. Table S1 shows Entrez gene IDs and probe set IDs of genes described in Fig. 4 A. Videos 1 and 2 show dynamics of OT-II T cells of the indicated genotypes in the GC and FM. Video 3 shows tracking of OT-II T cells that entered the GC-FM interface zone. Online supplemental materials are available at http://www.jem.org/cgi/content/full/jem.20131666/DC1.

We thank K.M. Ansel, M. Kitano, K. Kometani, S. Fagarasan, T.G. Phan, and T. Kurosaki for discussion, S. Kawamoto for anti-GFP staining, and IMS-RCAI core facilities for microarray analysis and cell sorting.

This work was supported by Research Fellowships of the Japan Society for the Promotion of Science for Young Scientists (S. Moriyama), RIKEN Special Postdoctoral Researcher Program (S. Moriyama), and the Ministry of Education, Culture, Sports, Science, and Technology of Japan (T. Okada).

The authors declare no competing financial interests.

Submitted: 7 August 2013
Accepted: 30 April 2014

REFERENCES

Allen, C.D., T. Okada, H.L. Tang, and J.G. Cyster. 2007. Imaging of germinal center selection events during affinity maturation. *Science*. 315:528–531. http://dx.doi.org/10.1126/science.1136736

Ansel, K.M., L.J. McHeyzer-Williams, V.N. Ngo, M.G. McHeyzer-Williams, and J.G. Cyster. 1999. In vivo–activated CD4 T cells upregulate CXC chemokine receptor 5 and reprogram their response to lymphoid chemokines. *J. Exp. Med.* 190:1123–1134. http://dx.doi.org/10.1084/jem.190.8.1123

Arnold, C.N., D.J. Campbell, M. Lipp, and E.C. Butcher. 2007. The germinal center response is impaired in the absence of T cell-expressed CXCR5. *Eur. J. Immunol.* 37:100–109. http://dx.doi.org/10.1002/eji.200636486

Cattoretti, G., J. Mandelbaum, N. Lee, A.H. Chaves, A.M. Mahler, A. Chadburn, R. Dalla-Favera, L. Pasqualucci, and A.J. MacLennan. 2009. Targeted disruption of the S1P2 sphingosine 1-phosphate receptor gene leads to diffuse large B-cell lymphoma formation. *Cancer Res.* 69:8686–8692. http://dx.doi.org/10.1158/0008-5472.CAN-09-1110

Du, W., N. Takuwa, K. Yoshioka, Y. Okamoto, K. Gonda, K. Sugihara, A. Fukamizu, M. Asano, and Y. Takuwa. 2010. $S1P_2$, the G protein-coupled receptor for sphingosine-1-phosphate, negatively regulates tumor angiogenesis and tumor growth in vivo in mice. *Cancer Res.* 70:772–781. http://dx.doi.org/10.1158/0008-5472.CAN-09-2722

Good-Jacobson, K.L., C.G. Szumilas, L. Chen, A.H. Sharpe, M.M. Tomayko, and M.J. Shlomchik. 2010. PD-1 regulates germinal center B cell survival and the formation and affinity of long-lived plasma cells. *Nat. Immunol.* 11:535–542. http://dx.doi.org/10.1038/ni.1877

Green, J.A., and J.G. Cyster. 2012. S1PR2 links germinal center confinement and growth regulation. *Immunol. Rev.* 247:36–51. http://dx.doi.org/10.1111/j.1600-065X.2012.01114.x

Green, J.A., K. Suzuki, B. Cho, L.D. Willison, D. Palmer, C.D. Allen, T.H. Schmidt, Y. Xu, R.L. Proia, S.R. Coughlin, and J.G. Cyster. 2011. The sphingosine 1-phosphate receptor $S1P_2$ maintains the homeostasis of germinal center B cells and promotes niche confinement. *Nat. Immunol.* 12:672–680. http://dx.doi.org/10.1038/ni.2047

Harada, Y., S. Tanaka, Y. Motomura, Y. Harada, S. Ohno, S. Ohno, Y. Yanagi, H. Inoue, and M. Kubo. 2012. The 3′ enhancer CNS2 is a critical regulator of interleukin-4-mediated humoral immunity in follicular helper T cells. *Immunity*. 36:188–200. http://dx.doi.org/10.1016/j.immuni.2012.02.002

Haynes, N.M., C.D. Allen, R. Lesley, K.M. Ansel, N. Killeen, and J.G. Cyster. 2007. Role of CXCR5 and CCR7 in follicular Th cell positioning and appearance of a programmed cell death gene-1high germinal center-associated subpopulation. *J. Immunol.* 179:5099–5108. http://dx.doi.org/10.4049/jimmunol.179.8.5099

Junt, T., K. Fink, R. Förster, B. Senn, M. Lipp, M. Muramatsu, R.M. Zinkernagel, B. Ludewig, and H. Hengartner. 2005. CXCR5-dependent seeding of follicular niches by B and Th cells augments antiviral B cell responses. *J. Immunol.* 175:7109–7116. http://dx.doi.org/10.4049/jimmunol.175.11.7109

Kitano, M., S. Moriyama, Y. Ando, M. Hikida, Y. Mori, T. Kurosaki, and T. Okada. 2011. Bcl6 protein expression shapes pre-germinal center B cell dynamics and follicular helper T cell heterogeneity. *Immunity*. 34:961–972. http://dx.doi.org/10.1016/j.immuni.2011.03.025

Linterman, M.A., R.J. Rigby, R.K. Wong, D. Yu, R. Brink, J.L. Cannons, P.L. Schwartzberg, M.C. Cook, G.D. Walters, and C.G. Vinuesa. 2009. Follicular helper T cells are required for systemic autoimmunity. *J. Exp. Med.* 206:561–576. http://dx.doi.org/10.1084/jem.20081886

Linterman, M.A., A. Liston, and C.G. Vinuesa. 2012. T-follicular helper cell differentiation and the co-option of this pathway by non-helper cells. *Immunol. Rev.* 247:143–159. http://dx.doi.org/10.1111/j.1600-065X.2012.01121.x

Lo, C.G., Y. Xu, R.L. Proia, and J.G. Cyster. 2005. Cyclical modulation of sphingosine-1-phosphate receptor 1 surface expression during lymphocyte recirculation and relationship to lymphoid organ transit. *J. Exp. Med.* 201:291–301. http://dx.doi.org/10.1084/jem.20041509

Lüthje, K., A. Kallies, Y. Shimohakamada, G.T. Belz, A. Light, D.M. Tarlinton, and S.L. Nutt. 2012. The development and fate of follicular helper T cells defined by an IL-21 reporter mouse. *Nat. Immunol.* 13:491–498. http://dx.doi.org/10.1038/ni.2261

MacLennan, A.J., P.R. Carney, W.J. Zhu, A.H. Chaves, J. Garcia, J.R. Grimes, K.J. Anderson, S.N. Roper, and N. Lee. 2001. An essential role for the H218/AGR16/Edg-5/LP(B2) sphingosine 1-phosphate receptor in neuronal excitability. *Eur. J. Neurosci.* 14:203–209. http://dx.doi.org/10.1046/j.0953-816x.2001.01634.x

Matloubian, M., C.G. Lo, G. Cinamon, M.J. Lesneski, Y. Xu, V. Brinkmann, M.L. Allende, R.L. Proia, and J.G. Cyster. 2004. Lymphocyte egress from thymus and peripheral lymphoid organs is dependent on S1P receptor 1. *Nature*. 427:355–360. http://dx.doi.org/10.1038/nature02284

McHeyzer-Williams, M., S. Okitsu, N. Wang, and L. McHeyzer-Williams. 2012. Molecular programming of B cell memory. *Nat. Rev. Immunol.* 12:24–34.

Miyao, T., S. Floess, R. Setoguchi, H. Luche, H.J. Fehling, H. Waldmann, J. Huehn, and S. Hori. 2012. Plasticity of $Foxp3^+$ T cells reflects promiscuous Foxp3 expression in conventional T cells but not reprogramming of regulatory T cells. *Immunity*. 36:262–275. http://dx.doi.org/10.1016/j.immuni.2011.12.012

Mombaerts, P., A.R. Clarke, M.A. Rudnicki, J. Iacomini, S. Itohara, J.J. Lafaille, L. Wang, Y. Ichikawa, R. Jaenisch, M.L. Hooper, et al. 1992. Mutations in T-cell antigen receptor genes α and β block thymocyte development at different stages. *Nature*. 360:225–231. http://dx.doi.org/10.1038/360225a0

Qi, H., J.L. Cannons, F. Klauschen, P.L. Schwartzberg, and R.N. Germain. 2008. SAP-controlled T-B cell interactions underlie germinal centre formation. *Nature*. 455:764–769. http://dx.doi.org/10.1038/nature07345

Ramiscal, R.R., and C.G.Vinuesa. 2013.T-cell subsets in the germinal center. *Immunol. Rev.* 252:146–155. http://dx.doi.org/10.1111/imr.12031

Reinhardt, R.L., H.E. Liang, and R.M. Locksley. 2009. Cytokine-secreting follicular T cells shape the antibody repertoire. *Nat. Immunol.* 10:385–393. http://dx.doi.org/10.1038/ni.1715

Shulman, Z., A.D. Gitlin, S. Targ, M. Jankovic, G. Pasqual, M.C. Nussenzweig, and G.D. Victora. 2013. T follicular helper cell dynamics in germinal centers. *Science*. 341:673–677. http://dx.doi.org/10.1126/science.1241680

Skoura, A., and T. Hla. 2009. Regulation of vascular physiology and pathology by the $S1P_2$ receptor subtype. *Cardiovasc. Res.* 82:221–228. http://dx.doi.org/10.1093/cvr/cvp088

Vinuesa, C.G., M.A. Linterman, C.C. Goodnow, and K.L. Randall. 2010. T cells and follicular dendritic cells in germinal center B-cell formation and selection. *Immunol. Rev.* 237:72–89. http://dx.doi.org/10.1111/j.1600-065X.2010.00937.x

Wang, X., B. Cho, K. Suzuki, Y. Xu, J.A. Green, J. An, and J.G. Cyster. 2011. Follicular dendritic cells help establish follicle identity and promote B cell retention in germinal centers. *J. Exp. Med.* 208:2497–2510. http://dx.doi.org/10.1084/jem.20111449